Title	Involvement of the Type IX Secretion System in Capnocytophaga ochracea Gliding Motility and Biofilm Formation
Author(s) Alternative	Kita, D; Shibata, S; Kikuchi, Y; Kokubu, E; Nakayama, K; Saito, A; Ishihara, K
Journal	Applied and environmental microbiology, 82(6): 1756-1766
URL	http://hdl.handle.net/10130/4075
Right	©2016, American Society for Microbiology

Involvement of the type IX secretion system in the gliding motility and biofilm formation of *Capnocytophaga ochracea*

Daichi Kita,[a] Satoshi Shibata,[b] Yuichiro Kikuchi,[c,d] Eitoyo Kokubu,[c,d] Koji Nakayama,[b] Atsushi Saito[a,d] and Kazuyuki Ishihara[c,d]#.

[a] Department of Periodontology, Tokyo Dental College, Tokyo, Japan; [b] Division of Microbiology and Oral Infection, Department of Molecular Microbiology and Immunology, Nagasaki University Graduate School of Biomedical Sciences, Nagasaki, Japan; [c] Department of Microbiology, Tokyo Dental College, Tokyo, Japan; [d] Oral Health Science Center, Tokyo Dental College, Tokyo, Japan.

Running Head: Involvement of T9SS in *C. ochracea* biofilms

#Address correspondence to Kazuyuki Ishihara, ishihara@tdc.ac.jp

Department of Microbiology, Tokyo Dental College, 2-1-14-6F Misaki-cho, Chiyoda-ku, Tokyo, 101-0061, Japan. Phone: +81 3 6380 9558.

Keywords: biofilm formation; gliding motility; protein secretion; gram-negative bacteria; T9SS

ABSTRACT

Capnocytophaga ochracea is a gram-negative, rod-shaped bacterium that demonstrates gliding motility when cultured on solid agar surfaces. *C. ochracea* possesses the ability to form biofilm. However, factors involved in biofilm formation by this bacterium are unclear. A type IX secretion system (T9SS) in *Flavobacterium johnsoniae* was shown to be involved in the transport of proteins (e.g., several adhesins) to the cell surface. Genes orthologous to those encoding T9SS proteins in *F. johnsoniae* have been identified in the genome of *C. ochracea*; therefore, the T9SS may be involved in biofilm formation by *C. ochracea*. Here we constructed three ortholog-deficient *C. ochracea* mutants lacking *sprB*, which encodes a gliding motility adhesin, or *gldK* or *sprT*, which encode T9SS proteins in *F. johnsoniae*. Gliding motility was lost in each mutant, suggesting that in *C. ochracea* the proteins encoded by *sprB*, *gldK*, and *sprT* are necessary for gliding motility and that SprB is transported to the cell-surface by the T9SS. The amount of crystal violet-associated biofilm, relative to wild-type, for the Δ*gldK*, Δ*sprT*, and Δ*sprB* strains at 48 h was 49%, 34%, and 65%, respectively. Confocal laser scanning and scanning electron microscopy revealed that the biofilms formed by wild-type *C. ochracea* were denser and biofilm cells were closer together-than those formed by the mutant strains. Together, these results indicate that proteins exported by the T9SS are key elements of the gliding motility and biofilm formation of *C. ochracea*.

INTRODUCTION

Capnocytophaga ochracea is a gram-negative, rod-shaped bacterium that demonstrates gliding motility when cultured on solid agar surfaces (1-3). *C. ochracea* was first isolated from human periodontitis lesions (4-6); however, subsequent studies have indicated that this bacterium is present in dental plaque from periodontally healthy sites (7). Although a recent metatranscriptome analysis has shown that putative virulence factors of *C. ochracea* are upregulated in patients with periodontitis (8), the role of *C. ochracea* in the pathogenesis and progression of periodontal disease remains controversial (9-13). *C. ochracea* is also reported to be involved in several systemic diseases and to produce an immunosuppressive factor (14, 15). *C. ochracea* has been implicated in focal infections such as sepsis and purpura fulminans (16, 17), and associations between high levels of antibodies to *C. ochracea* and coronary heart disease (18) and potential relationship with Sjögren's syndrome (19) have also been reported.

To clarify the involvement of *C. ochracea* in these diseases, the investigation of the colonization strategies by this bacterium is essential. *C. ochracea* colonizes tooth surfaces by forming a biofilm and synergizing its growth with that of *Fusobacterium nucleatum*, which acts as a bridge between antecedent bacteria on the tooth surface and late-colonizing periodontopathic bacteria (20). However, the factors involved in biofilm formation by this bacterium remain unknown. In *Escherichia coli*, it is thought that motility facilitates biofilm expansion by enabling growing cells to migrate across the surface on which they are growing (21). In *Pseudomonas aeruginosa*, flagella and pili are known to play important roles in aggregation of the bacterial cells and the formation of microcolonies (22).

Thus, we hypothesized that the gliding motility of *C. ochracea* is an important aspect of its biofilm formation.

Recently, a novel protein secretion system, the type IX secretion system (T9SS), was identified in *Porphyromonas gingivalis* and other members of phylum *Bacteroidetes*. For example, in *P. gingivalis*, which is a prominent periodontal pathogen, several T9SS proteins (e.g., PorK, PorL, PorT) were found to be crucial for the secretion of major proteases (23-26). T9SS proteins have also been found in *Flavobacterium johnsoniae* (phylum *Bacteroidetes*) (23, 25, 27, 28), and orthologous genes encoding T9SS proteins have been found in the genome of *C. ochracea* (28).

In *F. johnsoniae*, SprB (colony-spreading protein B) allows the bacterium to attach to agar and glass surfaces and move via gliding motility (29). *F. johnsoniae* mutants deficient in genes encoding T9SS proteins (e.g., *gldK*, *gldL*, *sprT*) are unable to attach to and glide across glass surfaces, presumably as a result of their inability to secrete SprB and other adhesins at their cell surface (30). Since *C. ochracea* harbors orthologous genes predicted to encode T9SS proteins such as GldK and SprT (28), it is possible that proteins exported by the T9SS are involved in the gliding motility and biofilm formation of *C. ochracea*.

Here we constructed *C. ochracea* mutants deficient in the genes orthologous to *gldK*, *sprT*, or *sprB* in *F. johnsoniae*, and investigated the role of the T9SS in gliding motility and biofilm formation. Our results indicated that proteins exported by the T9SS in *C. ochracea* are involved in gliding motility and biofilm formation.

MATERIALS AND METHODS

Bacterial strains, plasmids, and growth conditions. The bacterial strains and plasmids used in the present study are listed in Table 1. *C. ochracea* ATCC 27872 (wild-type) was cultured and maintained using standard methods on blood agar plates containing tryptic soy agar (Becton Dickinson, Sparks, MD) supplemented with hemin (5 μg/mL), menadione (0.5 μg/mL), and 10% horse blood (Nippon Bio-Test Laboratories, Tokyo, Japan) at 37°C under anaerobic conditions (80% N_2, 10% H_2, and 10% CO_2) in an anaerobic chamber (ANX-3, Hirasawa, Tokyo, Japan). *C. ochracea* mutants were cultured and maintained on blood agar plates containing 10 μg/mL erythromycin (Sigma-Aldrich, St. Louis, MO). *C. ochracea* strains were also grown in tryptic soy broth (Becton Dickinson) supplemented with hemin (5 μg/mL) and menadione (0.5 μg/mL) at 37°C under anaerobic conditions. *Escherichia coli* DH5α was grown at 37°C under anaerobic conditions in Luria-Bertani agar (Wako Pure Chemical Industries, Osaka, Japan), and the plasmid-transformed strains of *E. coli* were grown in Luria-Bertani agar containing 25 μg/mL kanamycin (Sigma-Aldrich).

Construction of Δ*gldK*, Δ*sprT*, and Δ*sprB* mutant strains. The genomic nucleotide sequence of *C. ochracea* ATCC 27872 was obtained from the GenBank database (accession number: NC_013162). The *C. ochracea* sequences of *gldK* and *sprT* (Coch_0809 and Coch_1748, respectively) were obtained from the National Center for Biotechnology Information database (www.ncbi.nlm.nih.gov/). The *C. ochracea* ortholog to the *F. johnsoniae* gene encoding the gliding motility protein SprB (31) was searched against the

whole genome sequence of *C. ochracea* in the National Center for Biotechnology Information database by means of a BLAST search. The *C. ochracea* DNA sequence obtained from the search was designated as *sprB* (Coch_0203).

The primers used in the present study are listed in Table 2. To construct the Δ*sprT* mutant, the upstream and downstream sequences of the target gene were amplified by means of the PCR from chromosomal DNA of *C. ochracea* ATCC 27872 with the primer pairs SprT-F1/SprT-R1 and SprT-F2/SprT-R2, respectively. The *ermF-ermAM* cassette was amplified from the pVA2198 plasmid by using the primers EMD2 and EMU2 (32). The *ermF-ermAM* cassette was inserted into the upstream and downstream fragments of the target genes by using an overlap extension PCR method (33).

Similarly, for the Δ*sprB* mutant, the upstream and downstream sequences of *sprB* were amplified by means of PCR from the chromosomal DNA with the primer pairs SprB-F1/SprB-R1 and SprB-F2/SprB-R2, respectively. For the Δ*gldK* mutant, the upstream and downstream sequences of the target gene were amplified by means of PCR from the chromosomal DNA with the primer pairs GldK-F1/GldK-R1 and GldK-F2/GldK-R2, respectively. The *ermF-ermAM* cassette was amplified from pVA2198 plasmid with the primers EMSprB-F and EMSprB-R (for *sprB*) or EMD2 and EMU2 (for *gldK*) and then inserted into the upstream and downstream fragments as described for the Δ*sprT* mutant.

The PCR-fused fragments from *sprT* and *sprB* were cloned into pCR2.1-TOPO, and the plasmids were transformed into *E. coli* DH5α. Transformants were selected on Luria-Bertani agar plates containing kanamycin (25 μg/mL). Recombinant plasmid DNA was isolated and digested with *Eco*RI. The obtained fragments (*sprT* or *sprB*) and the

PCR-fused fragments of *gldK* were introduced into *C. ochracea* ATCC 27872 by means of electroporation, as described below. Mid-logarithmic-phase *C. ochracea* ATCC 27872 was harvested from 100 mL of culture medium, washed three times with ice-cold distilled water, and suspended in 0.2 mL of 10% glycerol. Then, 10 μg of plasmid DNA was mixed with 40 μL of the cells and the mixture was incubated on ice for 1 min before being transferred to a 0.1-cm electroporation cuvette (Bio-Rad laboratories, Hercules, CA). Electroporation was performed with a Gene Pulser II (Bio-Rad) at settings of 1.8 kV, 25 μF, and 250 Ω. Immediately after electroporation, the cells were suspended in 1 mL of tryptic soy broth and incubated overnight at 37°C under anaerobic conditions. The cells were then plated on blood agar plates containing 10 μg/mL erythromycin and incubated for 5 to 7 days at 37°C under anaerobic conditions. Correct gene replacement in erythromycin-resistant mutants was confirmed by means of PCR (data not shown).

Growth properties of the mutant strains in liquid culture. *C. ochracea* strains were grown at 37°C for 2 days on blood agar plates and inoculated into tryptic soy broth. After reaching the early stationary phase, the culture was diluted with fresh medium to an OD_{660} of 0.1. Samples of the diluted cultures (10 mL) were then incubated at 37°C under anaerobic conditions. Bacterial growth was monitored by measuring optical density (OD) at 660 nm with a spectrophotometer (Mini Photo 518R; Taitec, Tokyo, Japan) at predetermined time points.

Microscopic observation of bacterial movement on solid agar and glass surfaces.

The movement of bacterial cells on solid agar surfaces (i.e., colony spreading) was examined by using phase-contrast microscopy as described previously with minor modifications (34). In brief, cells in the early stationary phase were suspended in fresh medium to an OD_{660} of 1.0. Five-microliter samples of the cell suspensions were then spotted on glass slides covered with a thin layer of tryptic soy agar (agar content, 3%) supplemented with hemin (5 μg/mL), menadione (0.5 μg/mL), and 0.1% yeast extract (TSAYE; Becton Dickinson). After incubation for 5 days at 37°C under anaerobic conditions, colony spreading was observed under a stereomicroscope (SMZ800; Nikon, Tokyo, Japan) equipped with a digital camera.

The movement of *C. ochracea* over a glass surface was also examined by means of phase-contrast microscopy. *C. ochracea* strains were grown for 2 days at 37°C under anaerobic conditions in tryptic soy broth supplemented with 0.1% yeast extract (TSBYE) and then dripped on tryptic soy agar supplemented with 0.1% yeast extract and incubated for 2 days at 37°C under anaerobic conditions. After incubation, the edges of the colonies were scraped off and resuspended in TSBYE. Tunnel slides were prepared as described previously by using 5-mm–thick double-sided tape (NW-5; Nichiban, Tokyo, Japan) to hold a glass coverslip above a glass slide (35). Cells suspended in TSBYE were introduced into the tunnel slides, and fresh TSBYE was used to wash away unattached cells. Cell motility was observed under an inverted microscope. Images were recorded at 5-s intervals for 10 min by using a charge-coupled device camera (Cool-SNAP EZ; Photometrics, Tucson, AZ) and analyzed using MetaMorph image analysis software (Molecular Devices, Downingtown, PA). Rainbow traces of cell movements were made by using ImageJ

software (version 1.44p; http://imagej.nih.gov/ij/) and the Color FootPrint macro (29).

Western blot analyses. To prepare a polyclonal antibody against *C. ochracea* SprB, a peptide corresponding to residues 5271–5284 with an added N-terminal cysteine residue (CAGDYWYVLKTHEDG) was synthesized by means of F-moc chemistry and conjugated to keyhole limpet hemocyanin by using maleimidobenzoic acid N-hydroxysuccinimide ester purchased from Sigma-Aldrich. Immunization of the peptide conjugate to rabbit, bleeding, and isolation of the serum were outsourced to Sigma-Aldrich. *C. ochracea* cells were grown to early stationary phase in tryptic soy broth at 37°C. The cells were then pelleted by centrifugation at 8000*g* for 30 min, and the culture supernatants were collected. The supernatants (20 μg of protein) were separated by means of sodium dodecyl sulfate-polyacrylamide gel electrophoresis (5% gels; Cosmo Bio, Tokyo, Japan) under reducing conditions. After electrophoresis, the proteins were transferred onto polyvinylidene difluoride membranes (Bio-Rad) and SprB was detected by using the polyclonal antibody (1:100 dilution).

Crystal violet biofilm formation assay. The biofilms formed by the *C. ochracea* strains were examined in 96-well polystyrene plates (Sumitomo Bakelite, Tokyo, Japan) as described previously with minor modifications (20). Stationary-phase cultures of *C. ochracea* were adjusted to an OD_{660} of 0.1 with fresh tryptic soy broth. Cells were then added to 96-well plates (100 μL/well) and incubated for 48 h at 37°C under anaerobic conditions. Following incubation, the wells were washed three times with 200 μL of

distilled water and stained with 50 µL of 0.1% crystal violet for 15 min at room temperature. After removing the crystal violet solution and washing each well twice with distilled water, the biomass-associated crystal violet was extracted with 200 µL of 99.5% ethanol. The extracted biomass-associated crystal violet (100 µL/well) was transferred to a new microtiter plate and the absorbance at OD_{595} was measured with a microplate reader (Spectra MAX M5e; Molecular Device, Sunnyvale, CA). Total biomass was calculated by using the following equation, which was described previously (36): total biomass = [absorbance of crystal-violet stained biofilm at OD_{595} / the absorbance of total growth (including biofilm and planktonic cells) at OD_{660}].

Confocal laser scanning microscopy analysis of biofilms. The biofilms produced by the *C. ochracea* strains were also examined by means of confocal laser scanning microscopy ~~as described previously with minor modifications (37)~~. One milliliter of cell suspension (OD_{660} of 0.1) was inoculated onto a plastic coverslip (Sumitomo Bakelite) in a 12-well polystyrene microtiter plate (BD Falcon, Franklin Lakes, NJ) at 37°C under anaerobic conditions. After 48 h, the medium was removed and the wells were washed three times with phosphate-buffered saline (PBS, 10 mM, pH 7.4) (2 mL/well) to remove unattached bacteria. The biofilms on the coverslips were fixed with 2% paraformaldehyde and 2.5% glutaraldehyde in PBS overnight at 4°C and stained with the nucleic acid stains SYTO9 and propidium iodide by using the LIVE/DEAD BacLight Bacterial Viability kit (Molecular Probes, Eugene, OR) according to the manufacturer's instructions. The biofilms were incubated in the dark at room temperature for 15 min, washed two times, and

observed by means of confocal laser scanning microscopy using a LSM5 DUO microscope (Carl Zeiss MicroImaging Inc., Göttingen, Germany) with a 63×/1.40 oil-immersion objective. A series of z-stack images were scanned in increments of 0.1 μm by using excitation wavelengths of 489 and 532 nm. The images were analyzed using Zen 2009 (Carl Zeiss MicroImaging Inc.) and Imaris 7.0.0 software (Bitplane AG, Zurich, Switzerland). Each z-stack image was further analyzed and quantified for biomass (total mass of living matter in a given unit area), average biofilm thickness, and maximum biofilm thickness by using the COMSTAT program (37).

Scanning electron microscopy analysis of biofilms. Samples were adjusted and incubated as described for the confocal laser scanning microscopy analysis. After 48 h, the medium was removed and the wells were washed once with PBS. Cells attached to the coverslips were fixed in 2% paraformaldehyde and 2.5% glutaraldehyde in PBS overnight at 4°C. The samples were washed twice with PBS and dehydrated in ethanol. The samples were then dried at the critical point of *t*-butyl alcohol, coated with gold/palladium by using a SC500A sputter coater (Bio-Rad), and observed under a scanning electron microscope (SU6600, Hitachi, Tokyo, Japan).

Biofilm stability. The stability of the biofilms produced by *C. ochracea* was examined by means of the crystal violet biofilm formation assay described above, with modification of the number of washes after removal of the medium, as described previously (~~39~~38).

Biofilm detachment assay. Enzymatic treatment was carried out as described previously with minor modifications (39, 40). Biofilms (produced by 100 µL of bacterial culture) were grown for 48 h in the wells of 96-well polystyrene microtiter plates as already described for the crystal violet biofilm formation assay. The biofilms were washed with 200 µL of distilled water and then treated overnight at 37°C with 200 µL of 0.5 mg/mL proteinase K (Roche Applied Sciences, Indianapolis, IN), DNase I (Roche Applied Sciences), or a carbohydrate-modifying agent sodium metaperiodate ($NaIO_4$) (Sigma-Aldrich) in PBS. Control wells received an equal volume of PBS. After treatment, the biofilms were washed twice with 200 µL of distilled water, stained with 50 µL crystal violet, and then quantitated as described for the crystal violet biofilm formation assay.

Microscopic observations of bacterial attachment to a glass surface. Attachment of the *C. ochracea* strains to a glass surface was examined by using tunnel slides as described previously (41). In brief, a stationary-phase culture of *C. ochracea* was adjusted to an OD_{660} of 0.5 with fresh tryptic soy broth, and 40 µL of the cell suspension was added to a tunnel slide. After 5 min, 200 µL of medium was added to wash away unattached cells. Cells attached to the slides were visualized under an inverted microscope (IX83; Olympus, Tokyo, Japan).

Autoaggregation assay. Autoaggregation of the *C. ochracea* strains was examined by using the assay described previously (20, 42). In brief, cells grown to stationary phase at 37°C under anaerobic conditions were washed twice with PBS and once with a

coaggregation buffer consisting of 1 mM Tris–HCl (pH 8.0), 0.1 mM $CaCl_2$, 0.1 mM $MgCl_2$, and 150 mM NaCl. Cells were re-suspended to an OD_{660} of 0.5 in the same buffer. One milliliter of each cell suspension was placed in a cuvette and the OD_{660} values at 0 and 120 min were determined with a spectrophotometer. The rate of autoaggregation was calculated by using the following equation: rate of autoaggregation = 100 – [(OD_{660} at 120 min/OD_{660} at 0 min) × 100].

Statistical analysis. Each experiment was performed independently at least twice. Results are expressed as mean values with standard deviations. One-way ANOVA with the Tukey–Kramer multiple comparisons test was used to determine differences between groups in the crystal violet biofilm formation assay. The Kruskal–Wallis test followed by Dunn's multiple comparisons test was used in the other experiments. $P < 0.05$ was considered statistically significant. Statistical calculations were performed with the Prism software package (version 6.04; GraphPad Software, La Jolla, CA).

RESULTS

Growth of the Δ*gldK*, Δ*sprT*, and Δ*sprB* mutants. To determine the effects of *gldK*, *sprT*, or *sprB* ortholog deficiency on the growth of *C. ochracea*, the growth of the wild-type and mutant strains of *C. ochracea* were monitored under anaerobic conditions at 37°C. There were no differences in the growth curves of the mutant strains compared with that of the wild-type strain up to the late log-phase. However, significant differences in growth were observed between the wild-type and mutant strains during late log and early stationary

phases (Fig. 1).

Movement of the mutant strains on solid agar and glass surfaces. To investigate the effects of *gldK*, *sprT*, or *sprB* ortholog deficiency on gliding motility, colony spreading of the wild-type and mutant strains on a solid agar surface was examined under a phase-contrast microscope (Fig. 2A). The wild-type strain formed colonies that exhibited marked spreading across the solid agar surface whereas the mutant strains formed colonies that exhibited little spreading. The movement of the wild-type and mutant strains on a glass surface was also examined. The wild-type strain exhibited movement over the glass surface but the mutant strains did not (Fig. 2B). Together, these results indicate that SprB is crucial for the movement of *C. ochracea* across solid surfaces and that SprB is secreted via the T9SS.

Involvement of SprT in the secretion of SprB. In *F. johnsoniae*, T9SS proteins such as GldK, GldL, and SprT are necessary for the secretion of the gliding motility adhesin SprB (30). Therefore, we examined the role of SprT in the secretion of SprB in *C. ochracea* by means of Western blotting (Fig. 3). SprB was detected in the culture supernatant of the wild-type strain but not in the supernatant of the Δ*sprT* mutant, indicating that the Δ*sprT* mutant did not secrete SprB. The size of the band detected was approximately equal to the estimated molecular mass of SprB (564410.11 Da).

Biofilm formation by the mutant strains. Each mutant strain was significantly

attenuated in biofilm formation compared with the wild-type strain (Fig. 4A, B). The amounts of crystal violet-associated biomass for the Δ*gldK*, Δ*sprT*, and Δ*sprB* strains at 48 h were 49%, 34%, and 65% that for the wild-type strain, respectively, indicating that the T9SS was involved in biofilm formation. To further investigate the effects of *gldK*, *sprT*, or *sprB* ortholog deficiency on biofilm formation, we examined the three-dimensional structure of the biofilms by means of confocal laser scanning microscopy and the COMSTAT program. The wild-type biofilm appeared denser than the mutant biofilms (Fig. 4C) and the biomass, average thickness, and maximum thickness of the Δ*gldK*, Δ*sprT* and Δ*sprB* biofilms were significantly lower than those of the wild-type biofilm (Fig. 4D). Furthermore, the amount of crystal violet-associated biomass and the average and maximum thickness of the Δ*gldK* and Δ*sprT* biofilm were significantly lower than those of the Δ*sprB* biofilm (Fig. 4A, D). Together these results indicate not only that SprB secreted via the T9SS is involved in biofilm formation, but also that because biofilm formation was not completely attenuated other proteins are also involved in biofilm formation by *C. ochracea*. To avoid the effect of the confounder as much as we could, the amount of crystal-violet-stained biofilm produced by the wild-type and each mutant of *C. ochracea* after 48 h incubation was adjusted by the total growth measured by absorbance at 660 nm (including biofilm and planktonic cells), and there were still significant differences between the wild-type and each mutant (data not shown).

Scanning electron microscope analysis of the structure of the biofilm. Bacterial biofilms are usually supported by a matrix of biopolymers known as extracellular

polymeric substances (EPSs) (43). We next used a scanning electron microscope to analyze the structure of the biofilms formed by the *C. ochracea* strains. The wild-type strain formed a denser biofilm with the cells packed closer together than did the mutant strains. (Fig. 5).

Stability of the biofilms produced by the mutants strains. To investigate the stability of the biofilms produced by the mutants, the crystal violet biofilm formation assay was used but with different amounts of washing (Fig. 6). After a single wash, the decrease in the amount of crystal violet-associated biomass was significantly greater for the Δ*gldK* and Δ*sprT* strains than it was for the wild-type strain. After three washes, the decreases in the amount of crystal violet-associated biomass for the all mutant strains were significantly greater than that for the wild-type strain. These results indicate that deletion of *gldK*, *sprT* or *sprB* in *C. ochracea* reduces the stability of the *C. ochracea* biofilm.

Enzyme treatment of the biofilms. EPSs can be proteins, nucleic acids, or polysaccharides (44, 45). Therefore, to further characterize the structure of the biofilm, we treated mature *C. ochracea* biofilms with proteinase K, DNase I, or $NaIO_4$. Treatment with proteinase K significantly reduced the amount of biofilm produced by the wild-type, Δ*sprT*, and Δ*sprB* strains, indicating that biofilms produced by these strains were predominantly proteinaceous (Fig. 7). DNaseI treatment reduced slightly the amount of biofilm but the amount was not significant.

Attachment to a glass surface and autoaggregation of the mutant strains. The

adherence of bacteria to a solid surface is the first step in biofilm formation (44). Therefore, the effects of *gldK*, *sprT*, or *sprB* ortholog deficiency on the ability of *C. ochracea* to attach to a glass surface was examined by means of phase-contrast microscopy. Wild-type and Δ*sprT* strains exhibited comparable adherence to the glass surface; however, the Δ*gldK* and the Δ*sprB* strains exhibited significantly less adherence compared with that of wild-type cells (Fig. 8).

Autoaggregation of the mutant strains was also examined because it may play an important role in cellular adherence and biofilm formation (46). However, the autoaggregation rates of the wild-type, Δ*gldK*, Δ*sprT*, and Δ*sprB* strains were 6.7% ± 4.3%, 2.8% ± 2.5%, 5.7% ± 2.2%, and 7.0% ± 1.3%, respectively (data are presented as means ± SD), indicating that autoaggregation is unaffected by deletion of *sprT* or *sprB*.

DISCUSSION

Bacterial surface molecules such as proteins are important for the attachment of bacterial cells to surfaces and for biofilm formation because they interact directly with biotic or abiotic surfaces (47, 48). T9SS is a major protein transport system for bacteria in the phylum *Bacteroidetes*, and it has been shown to be involved in the secretion of surface motility adhesins in *F. johnsoniae* (30). Here we demonstrated that SprB, GldK and SprT were involved in biofilm formation of *C. ochracea*.

Motility is an important factor for biofilm formation by gram-negative bacteria. In *E. coli*, highly motile strains display biofilm structures that extend vertically, whereas strains with less motility display smoother microcolonies (49). As *C. ochracea* has gliding activity,

it is possible that the activity play an important role to colonize on the tooth surface. A recent study in *Flavobacterium* spp. suggests that gliding motility is important for bacterial attachment to and colonization of plant surfaces (50). In the present study, we showed that deletion of the *C. ochracea* orthologs of *gldK*, *sprT*, and *sprB* resulted in defective gliding motility on solid surfaces (Fig. 2). In *F. johnsoniae*, SprB is transported by the T9SS, is propelled along a left-handed helical loop on the cell surface, and is involved in gliding motility (25, 29). Similary, the results of the present study indicate that SprB is also transported by the T9SS (Fig. 3) and is involved in gliding motility in *C. ochracea*. The reduction in biofilm formation relative to that of the wild-type strain was greater in strains Δ*gldK* and Δ*sprT* than in Δ*sprB*, even after correction for bacterial growth (Fig. 4), suggesting that gliding motility is partly involved in biofilm formation by *C. ochracea* and that proteins exported by the T9SS other than SprB are involved in biofilm formation.

Many bacteria that belong to the phylum *Bacteroidetes* secrete extracellular and surface proteins via T9SS. The present data indicated GldK and SprT, which are the component of T9SS (30), involved in biofilm formation. Several proteins with a conserved C-terminal domain (CTD) region, which is required for secretion by T9SS, were detected in genome sequence of *C. ochracea* (data not shown). The different protein showed similar reduction in biofilm formation (Fig. 4) and adherence (Fig. 8), suggesting that the protein secreted by T9SS involves biofilm formation. In Fig. 4, reduction level of the Δ*gldK* mutant was somewhat low compared of that of Δ*sprT* mutant. GldK is required for secretion by the *F. johnsoniae* T9SS (B). SprT also have important roles in T9SS-mediated secretion, and cells with mutations in the genes encoding these proteins are severely but incompletely

deficient in secretion. (A, B, C). The difference in reduction of average biomass and thickness of biofilm agreed the incompletely deficient in secretion in Δ*sprT* mutant. These results suggest that GldK and SprT indirectly involved biofilm formation via secretion of the proteins including SprB by T9SS (Fig. 9) although further study by proteomics analysis is necessary to clarify the location of these proteins in 3 dimensional structure of T9SS.

Bacterial adherence is another important factor for biofilm formation (51). Previous studies have shown that a Δ*gldK* or Δ*sprT* mutant of *F. johnsoniae* failed to attach to a glass surface (25, 30). In contrast, in the present study, the ability of the Δ*gldK* mutant of *C. ochracea* to adhere to a glass surface decreased, but the decrease was much smaller than the decrease of the Δ*gldK* mutant of *F. johnsoniae*. In addition to that, the ability of the Δ*sprT* mutant of *C. ochracea* to adhere to a glass surface was comparable with that of the wild-type strain (Fig. 8), suggesting that *C. ochracea* possesses other secretion systems that translocate adhesins to the cell surface and *C. ochracea* GldK and SprT are involved more in the maintenance of the three-dimensional architecture of the biofilm than in bacterial adhesion. Our results also indicate that autoaggregation does not play a major role in biofilm formation by *C. ochracea*.

Generally, biofilms cannot easily be removed by fluid shear stress (44). However, in the present study, the amount of Δ*gldK* and Δ*sprT* mutants biofilms remaining was dramatically decreased after washing compared with the wild-type biofilm (Fig. 6). This result further confirms that in *C. ochracea* GldK and SprT ~~is~~ are involved in the maintenance of the biofilm architecture. In contrast, the amount of biofilm formed by the Δ*sprB* mutant was significantly decreased after washing three times but not after one wash

(Figs. 5–7), suggesting that in *C. ochracea* SprB is also involved in the maintenance of the biofilm architecture. However, the degree of involvement of SprB in the maintenance of the biofilm architecture is likely less than that of GldK or SprT, which is reasonable given that SprB is one of the proteins secreted via the T9SS. The present results also indicate that there are other substances secreted via the T9SS that are crucial for the maintenance of the biofilm architecture because biofilm formation was not completely attenuated in the mutants.

EPSs provide bacterial biofilms mechanical stability, keep biofilm cells in close proximity, mediate bacterial adhesion to surfaces, and form a cohesive, three-dimensional polymer network that interconnects and transiently immobilizes cells within the biofilm (43). Our scanning electron microscope analysis indicated that the wild-type biofilm was denser and biofilm cells were closer together ~~and had a more prominent matrix-like structure~~ than did the all mutants biofilms (Fig. 5). As described above, EPS keep biofilm cells in close proximity. Therefore these results suggest the involvement of EPS in differences in each biofilm. Moreover, treatment with proteinase K significantly reduced the total mass of the *C. ochracea* biofilm, whereas treatment with DNase I or $NaIO_4$ did not (Fig. 7), indicating that the main components of the biofilm were proteinaceous and that the proteinaceous substances were responsible for the strength and amount of biofilm produced by *C. ochracea* (Fig. 9). Since the T9SS is a protein secretion system, these results suggest that in addition to SprB other proteins exported by the T9SS are involved in biofilm formation. We treated biofilm with $NaIO_4$ to investigate the existence of polysaccharide in EPS, because it was reported that *C. ochracea* produces the exopolysaccharide containing

large amounts of mannose with lesser quantities of glucose, galactose, glucuronic acid, and glucosamine (52, 53), and $NaIO_4$ oxidizes an acidic polysaccharide and destruct the the mannose residues of it (54). The results suggest that the mannose rich exopolysaccharide was not major architecture of the biofilm. However, the results are not enough to ruled out involvement of other types of polysaccharides in biofilm architecture, further analysis is required to investigate them by a staining procedure and so on in the future.

Altered biofilm formation by T9SS-component mutants has been reported in *Tannerella forsythia*, which is an important pathogen in periodontal disease (36, 57, 58). These mutants lacked the *T. forsythia* surface layer (S-layer), which contains the cell-surface glycoproteins TfsA and TfsB (36, 58). The S-layer is known to be involved in *T. forsythia* adhesion to and invasion of host cells and in *T. forsythia*-mediated suppression of proinflammatory cytokine expression. A *T. forsythia* mutant deficient in the S-layer exhibited decreased hemagglutination and increased biofilm formation (48, 49). These findings contradict our present observation that the amount of biofilm formed by the mutant *C. ochracea* strains was less than that formed by the wild-type strain. This difference may be a result of whether or not the bacteria possesses an S-layer, but further analysis is required to understand the differences in biofilm formation between the *T. forsythia* and *C. ochracea* mutant strains. Analysis of the biofilms formed by T9SS-component mutants of other members of phylum *Bacteroidetes* may also help us to understand the detailed role of the T9SS in biofilm formation. Taken together, T9SS of *C. ochracea* may play a key role in colonization in oral cavity by *C. ochracea.*

In the present study, we clarified the involvement of the T9SS in *C. ochracea* biofilm

formation. *C. ochracea* is found mainly in the oral cavity, and is known to coaggregate in human dental plaque biofilm with *F. nucleatum* (1, 20, 51), which is a core bacterium for the growth of periodontopathic bacteria including *Porphyromonas*, *Fusobacterium*, and *Prevotella* spp., and it was recently reported that *Capnocytophaga* spp. increase their dominance within the dental plaque bacterial community as dental plaque matures (59). Furthermore, a number of other bacteria, including major pathogens of periodontitis, have been found to harbor T9SS-related genes (28). Therefore, inhibitors of the T9SS represent a potential means of controlling the development of periodontopathic biofilm. Further clarification of the roles of T9SS in periodontal pathogens is now needed.

ACKNOWLEDGMENTS

The authors thank Kazuko Okamoto-Shibayama for her helpful discussions, and Tomomi Kawana, Yoshiaki Kitazawa, and Katsumi Tadokoro for their technical assistance. This work was supported in part by a Grant-in-Aid for Scientific Research (C) 25463228 (to AS) and (C) 24592778 (to KI) from the Japan Society for the Promotion of Science.

REFERENCES

1. **Mavrommatis K, Gronow S, Saunders E, Land M, Lapidus A, Copeland A, Glavina Del Rio T, Nolan M, Lucas S, Chen F, Tice H, Cheng JF, Bruce D, Goodwin L, Pitluck S, Pati A, Ivanova N, Chen A, Palaniappan K, Chain P, Hauser L, Chang YJ, Jeffries CD, Brettin T, Detter JC, Han C, Bristow J, Goker M, Rohde M, Eisen JA, Markowitz V, Kyrpides NC, Klenk HP,**

Hugenholtz P. 2009. Complete genome sequence of *Capnocytophaga ochracea* type strain (VPI 2845). Stand Genomic Sci **1:**101-109.

2. **Leadbetter E, Holt S, Socransky S.** 1979. Capnocytophaga: new genus of gram-negative gliding bacteria. I. General characteristics, taxonomic considerations and significance. Arch microbiol **122:**9-16.

3. **Poirier TP, Tonelli SJ, Holt SC.** 1979. Ultrastructure of gliding bacteria: scanning electron microscopy of *Capnocytophaga sputigena*, *Capnocytophaga gingivalis*, and *Capnocytophaga ochracea*. Infect Immun **26:**1146-1158.

4. **Newman MG, Socransky SS.** 1977. Predominant cultivable microbiota in periodontosis. J Periodontal Res **12:**120-128.

5. **Slots J.** 1979. Subgingival microflora and periodontal disease. J Clin Periodontol **6:**351-382.

6. **Williams BL, Ebersole JL, Spektor MD, Page RC.** 1985. Assessment of serum antibody patterns and analysis of subgingival microflora of members of a family with a high prevalence of early-onset periodontitis. Infect Immun **49:**742-750.

7. **Kobayashi N, Ishihara K, Sugihara N, Kusumoto M, Yakushiji M, Okuda K.** 2008. Colonization pattern of periodontal bacteria in Japanese children and their

mothers. J Periodontal Res **43:**156-161.

8. **Duran-Pinedo AE, Chen T, Teles R, Starr JR, Wang X, Krishnan K, Frias-Lopez J.** 2014. Community-wide transcriptome of the oral microbiome in subjects with and without periodontitis. ISME J **8:**1659-1672.

9. **Kumar PS, Griffen AL, Barton JA, Paster BJ, Moeschberger ML, Leys EJ.** 2003. New bacterial species associated with chronic periodontitis. J Dent Res **82:**338-344.

10. **Paster BJ, Boches SK, Galvin JL, Ericson RE, Lau CN, Levanos VA, Sahasrabudhe A, Dewhirst FE.** 2001. Bacterial diversity in human subgingival plaque. J Bacteriol **183:**3770-3783.

11. **Colombo AP, Haffajee AD, Dewhirst FE, Paster BJ, Smith CM, Cugini MA, Socransky SS.** 1998. Clinical and microbiological features of refractory periodontitis subjects. J Clin Periodontol **25:**169-180.

12. **Moore WE, Moore LV.** 1994. The bacteria of periodontal diseases. Periodontol 2000 **5:**66-77.

13. **Dzink JL, Socransky SS, Haffajee AD.** 1988. The predominant cultivable microbiota of active and inactive lesions of destructive periodontal diseases. J Clin

Periodontol **15:**316-323.

14. **Bolton RW, Kluever EA, Dyer JK.** 1985. In vitro immunosuppression mediated by an extracellular polysaccharide from *Capnocytophaga ochracea*. Influence of macrophages. J Periodontal Res **20:**251-259.

15. **Ochiai K, Senpuku H, Kurita-Ochiai T.** 1998. Purification of immunosuppressive factor from *Capnocytophaga ochracea*. J Med Microbiol **47:**1087-1095.

16. **Desai SS, Harrison RA, Murphy MD.** 2007. *Capnocytophaga ochracea* causing severe sepsis and purpura fulminans in an immunocompetent patient. J Infect **54:**e107-109.

17. **Piau C, Arvieux C, Bonnaure-Mallet M, Jolivet-Gougeon A.** 2013. *Capnocytophaga* spp. involvement in bone infections: a review. Int J Antimicrob Agents **41:**509-515.

18. **Beck JD, Eke P, Heiss G, Madianos P, Couper D, Lin D, Moss K, Elter J, Offenbacher S.** 2005. Periodontal disease and coronary heart disease: a reappraisal of the exposure. Circulation **112:**19-24.

19. **Szymula A, Rosenthal J, Szczerba BM, Bagavant H, Fu SM, Deshmukh US.** 2014. T cell epitope mimicry between Sjogren's syndrome Antigen A (SSA)/Ro60

and oral, gut, skin and vaginal bacteria. Clin Immunol **152:**1-9.

20. **Okuda T, Okuda K, Kokubu E, Kawana T, Saito A, Ishihara K.** 2012. Synergistic effect on biofilm formation between *Fusobacterium nucleatum* and *Capnocytophaga ochracea*. Anaerobe **18:**157-161.

21. **Pratt LA, Kolter R.** 1998. Genetic analysis of *Escherichia coli* biofilm formation: roles of flagella, motility, chemotaxis and type I pili. Mol Microbiol **30:**285-293.

22. **Costerton JW, Stewart PS, Greenberg EP.** 1999. Bacterial biofilms: a common cause of persistent infections. Science **284:**1318-1322.

23. **Sato K, Yukitake H, Narita Y, Shoji M, Naito M, Nakayama K.** 2013. Identification of *Porphyromonas gingivalis* proteins secreted by the Por secretion system. FEMS Microbiol Lett **338:**68-76.

24. **Shoji M, Sato K, Yukitake H, Kondo Y, Narita Y, Kadowaki T, Naito M, Nakayama K.** 2011. Por secretion system-dependent secretion and glycosylation of *Porphyromonas gingivalis* hemin-binding protein 35. PLoS One **6:**e21372.

25. **Sato K, Naito M, Yukitake H, Hirakawa H, Shoji M, McBride MJ, Rhodes RG, Nakayama K.** 2010. A protein secretion system linked to *bacteroidete* gliding motility and pathogenesis. Proc Natl Acad Sci U S A **107:**276-281.

26. **Sato K, Sakai E, Veith PD, Shoji M, Kikuchi Y, Yukitake H, Ohara N, Naito M, Okamoto K, Reynolds EC, Nakayama K.** 2005. Identification of a new membrane-associated protein that influences transport/maturation of gingipains and adhesins of *Porphyromonas gingivalis*. J Biol Chem **280:**8668-8677.

27. **Kharade SS, McBride MJ.** 2014. *Flavobacterium johnsoniae* chitinase ChiA is required for chitin utilization and is secreted by the type IX secretion system. J Bacteriol **196:**961-970.

28. **McBride MJ, Zhu Y.** 2013. Gliding motility and Por secretion system genes are widespread among members of the phylum *bacteroidetes*. J Bacteriol **195:**270-278.

29. **Nakane D, Sato K, Wada H, McBride MJ, Nakayama K.** 2013. Helical flow of surface protein required for bacterial gliding motility. Proc Natl Acad Sci U S A **110:**11145-11150.

30. **Shrivastava A, Johnston JJ, van Baaren JM, McBride MJ.** 2013. *Flavobacterium johnsoniae* GldK, GldL, GldM, and SprA are required for secretion of the cell surface gliding motility adhesins SprB and RemA. J Bacteriol **195:**3201-3212.

31. **Nelson SS, Bollampalli S, McBride MJ.** 2008. SprB is a cell surface component of the *Flavobacterium johnsoniae* gliding motility machinery. J Bacteriol

190:2851-2857.

32. **Fletcher HM, Schenkein HA, Morgan RM, Bailey KA, Berry CR, Macrina FL.** 1995. Virulence of a *Porphyromonas gingivalis* W83 mutant defective in the prtH gene. Infect Immun **63:**1521-1528.

33. **Shevchuk NA, Bryksin AV, Nusinovich YA, Cabello FC, Sutherland M, Ladisch S.** 2004. Construction of long DNA molecules using long PCR-based fusion of several fragments simultaneously. Nucleic Acids Res **32:**e19.

34. **Ji X, Bai X, Li Z, Wang S, Guan Z, Lu X.** 2013. A novel locus essential for spreading of *Cytophaga hutchinsonii* colonies on agar. Appl Microbiol Biotechnol **97:**7317-7324.

35. **Shrivastava A, Rhodes RG, Pochiraju S, Nakane D, McBride MJ.** 2012. *Flavobacterium johnsoniae* RemA is a mobile cell surface lectin involved in gliding. J Bacteriol **194:**3678-3688.

36. **Narita Y, Sato K, Yukitake H, Shoji M, Nakane D, Nagano K, Yoshimura F, Naito M, Nakayama K.** 2014. Lack of a surface layer in *Tannerella forsythia* mutants deficient in the type IX secretion system. Microbiology **160:**2295-2303.

37. **Heydorn A, Nielsen AT, Hentzer M, Sternberg C, Givskov M, Ersboll BK,**

Molin S. 2000. Quantification of biofilm structures by the novel computer program COMSTAT. Microbiology **146:**2395-2407.

38. **Nilsson M, Chiang WC, Fazli M, Gjermansen M, Givskov M, Tolker-Nielsen T.** 2011. Influence of putative exopolysaccharide genes on *Pseudomonas putida* KT2440 biofilm stability. Environ Microbiol **13:**1357-1369.

39. **Hansen H, Bjelland AM, Ronessen M, Robertsen E, Willassen NP.** 2014. LitR Is a Repressor of syp Genes and Has a Temperature-Sensitive Regulatory Effect on Biofilm Formation and Colony Morphology in *Vibrio* (*Aliivibrio*) *salmonicida*. Appl Environ Microbiol **80:**5530-5541.

40. **Kaplan JB, Velliyagounder K, Ragunath C, Rohde H, Mack D, Knobloch JK, Ramasubbu N.** 2004. Genes involved in the synthesis and degradation of matrix polysaccharide in *Actinobacillus actinomycetemcomitans* and *Actinobacillus pleuropneumoniae* biofilms. J Bacteriol **186:**8213-8220.

41. **Weiss DG.** 2005. Video-Enhanced Contrast Microscopy, p. 57-65. *In* Ceils JE, Hunter T, Carter N, Shotton D, Small JV, Simons K (ed.), Cell Biology: A laboratory handbook, 3rd ed, vol. 3. Academic Press, San Diego.

42. **Honma K, Mishima E, Inagaki S, Sharma A.** 2009. The OxyR homologue in *Tannerella forsythia* regulates expression of oxidative stress responses and biofilm

formation. Microbiology **155:**1912-1922.

43. **Flemming HC, Wingender J.** 2010. The biofilm matrix. Nat Rev Microbiol **8:**623-633.

~~44~~. **Palmer J, Flint S, Brooks J.** 2007. Bacterial cell attachment, the beginning of a biofilm. J Ind Microbiol Biotechnol **34:**577-588.

45. **Monds RD, O'Toole GA.** 2009. The developmental model of microbial biofilms: ten years of a paradigm up for review. Trends Microbiol **17:**73-87.

46. **Basson A, Flemming LA, Chenia HY.** 2008. Evaluation of adherence, hydrophobicity, aggregation, and biofilm development of *Flavobacterium johnsoniae*-like isolates. Microb Ecol **55:**1-14.

47. **Rosan B, Lamont RJ.** 2000. Dental plaque formation. Microbes Infect **2:**1599-1607.

48. **Chagnot C, Zorgani MA, Astruc T, Desvaux M.** 2013. Proteinaceous determinants of surface colonization in bacteria: bacterial adhesion and biofilm formation from a protein secretion perspective. Front Microbiol **4:**303.

49. **Wood TK, Gonzalez Barrios AF, Herzberg M, Lee J.** 2006. Motility influences

biofilm architecture in *Escherichia coli*. Appl Microbiol Biotechnol **72:**361-367.

50. **Kolton M, Frenkel O, Elad Y, Cytryn E.** 2014. Potential role of Flavobacterial gliding-motility and type IX secretion system complex in root colonization and plant defense. Mol Plant Microbe Interact **27:**1005-1013.

51. **Kolenbrander PE, Palmer RJ, Jr., Periasamy S, Jakubovics NS.** 2010. Oral multispecies biofilm development and the key role of cell-cell distance. Nat Rev Microbiol **8:**471-480.

52. **Dyer JK, Bolton RW.** 1985. Purification and chemical characterization of an exopolysaccharide isolated from *Capnocytophaga ochracea*. Can J Microbiol **31:**1-5.

53. **Bolton RW, Dyer JK.** 1983. Suppression of murine lymphocyte mitogen responses by exopolysaccharide from *Capnocytophaga ochracea*. Infect Immun **39:**476-479.

54. **Le Ba N, Jann B, Jann K.** 1971. Immunochemistry of K antigens of *Escherichia coli*. The K29 antigen of *E. coli* 09:K29(A):H. Eur J Biochem **21:**226-234.

55. **Callebaut I, Gilges D, Vigon I, Mornon JP.** 2000. HYR, an extracellular module involved in cellular adhesion and related to the immunoglobulin-like fold. Protein Sci **9:**1382-1390.

56. **Loehfelm TW, Luke NR, Campagnari AA.** 2008. Identification and characterization of an *Acinetobacter baumannii* biofilm-associated protein. J Bacteriol **190:**1036-1044.

57. **Sharma A.** 2010. Virulence mechanisms of *Tannerella forsythia*. Periodontol 2000 **54:**106-116.

58. **Tomek MB, Neumann L, Nimeth I, Koerdt A, Andesner P, Messner P, Mach L, Potempa JS, Schaffer C.** 2014. The S-layer proteins of *Tannerella forsythia* are secreted via a type IX secretion system that is decoupled from protein O-glycosylation. Mol Oral Microbiol **29:**307-320.

59. **Takeshita T, Yasui M, Shibata Y, Furuta M, Saeki Y, Eshima N, Yamashita Y.** 2015. Dental plaque development on a hydroxyapatite disk in young adults observed by using a barcoded pyrosequencing approach. Sci Rep **5:**8136.

A. **Sato K, Naito M, Yukitake H, Hirakawa H, Shoji M, McBride MJ, Rhodes RG, Nakayama K.** 2010. A protein secretion system linked to bacteroidete gliding motility and pathogenesis. Proc Natl Acad Sci U S A **107:**276 –281. http://dx.doi.org/10.1073/pnas.0912010107.

B. **Shrivastava A, Johnston JJ, van Baaren JM, McBride MJ.** 2013. *Flavo- bacterium*

johnsoniae GldK, GldL, GldM, and SprA are required for secre- tion of the cell-surface gliding motility adhesins SprB and RemA. J Bacte- riol **195:**3201–3212. http://dx.doi.org/10.1128/JB.00333-13.

C. **Rhodes RG, Samarasam MN, Van Groll EJ, McBride MJ.** 2011. Muta- tions in *Flavobacterium johnsoniae sprE* result in defects in gliding motility and protein secretion. J Bacteriol **193:**5322–5327. http://dx.doi.org/10 .1128/JB.05480-11.

Figure legends

Fig. 1. Growth curves of wild-type and ortholog deficient mutant strains of *Capnocytophaga ochracea*.

Wild-type *C. ochracea* ATCC 27872 (WT) (black closed squares), Δ*gldK* mutant (open light-gray squares), Δ*sprT* mutant (open gray circles), and Δ*sprB* mutant (closed dark-gray triangles) were grown in tryptic soy broth supplemented with hemin and menadione at 37°C under anaerobic conditions. Data are presented as means ± SD ($n \geq 8$). ***$P < 0.001$ (Δ*gldK* mutant vs. WT), $^{\ddagger}P < 0.01$ (Δ*sprT* mutant vs. WT), and $^{\S}P < 0.05$ (Δ*sprB* mutant vs. WT)

Fig. 2. Effects of *gldK*, *sprT*, or *sprB* ortholog deficiency on gliding motility in *Capnocytophaga ochracea*.

(A) Effects of *gldK*, *sprT*, or *sprB* ortholog deletion on colony spreading on a solid agar surface. Representative photographs of the colonies and photomicrographs of the edges of the colonies of each strain are shown. The black arrow indicates cells spreading away from the colony. Scale bars, 100 μm. (B) Effects of *gldK*, *sprT*, or *sprB* ortholog deletion on gliding motility on a glass surface. Rainbow traces of cell movements were created with image analysis software. Non-motile cells are shown in white. Scale bars, 10 μm. WT, wild-type *C. ochracea* ATCC 27872; Δ*gldK*, *gldK* ortholog-deficient *C. ochracea* mutant; Δ*sprT*, *sprT* ortholog-deficient *C. ochracea* mutant; Δ*sprB*, *sprB* ortholog-deficient *C. ochracea* mutant.

Fig. 3. Western blot analysis of the culture supernatant of wild-type *Capnocytophaga ochracea* ATCC 27872 and of the Δ*sprT* mutant. The culture supernatants were subjected to sodium dodecyl sulfate-polyacrylamide gel electrophoresis and western blot analysis with an antibody against SprB. Lanes: M, molecular size marker; WT, wild-type *C. ochracea* ATCC 27872; Δ*sprT*, *sprT* ortholog-deficient *C. ochracea* mutant. The size of the band observed for wild-type *C. ochracea* was approximately equal to the estimated molecular mass of sprB (564410.11 Da).

Fig. 4. Effects of *gldK*, *sprT*, or *sprB* ortholog deficiency on biofilm formation by *Capnocytophaga ochracea*.

(A) Cells were incubated at 37°C under anaerobic conditions for 48 h and the amount of biofilm produced was quantified by measuring OD_{595} following crystal violet staining. Total biomass was calculated by using the following equation: Total biomass = [absorbance of crystal violet stained biofilm at OD_{595} / the absorbance of total growth (including biofilm and planktonic cells) at OD_{660}]. Data are presented as mean ± SD (n = 18). *P < 0.05, ***P < 0.001 (B) Representative images of the results of the crystal violet biofilm formation assay. (C) Confocal laser scanning microscopy analysis of *C. ochracea* biofilms. *C. ochracea* strains incubated at 37°C under anaerobic conditions for 48 h were stained with the nucleic acid stains SYTO9 and propidium iodide. Images are presented as orthographic projections. (D) COMSTAT analyses of the three-dimensional structures of the biofilms produced by the wild-type and mutant strains of *C. ochracea*. Data are presented as means ± SD (n = 19). *P < 0.05, **P < 0.01, ***P < 0.001 WT, wild-type *C. ochracea* ATCC

27872; Δ*gldK*, *gldK* ortholog-deficient *C. ochracea* mutant; Δ*sprT*, *sprT* ortholog-deficient *C. ochracea* mutant; Δ*sprB*, *sprB* ortholog-deficient *C. ochracea* mutant. Scale bars, 10 μm.

Fig. 5. Scanning electron microscopy analysis of the structures of the *C. ochracea* biofilms. The biofilms were cultured at 37°C for 48 h before fixation. Scale bars, 20 μm for ×2000 magnification and 2 μm for ×20000 magnification. WT, wild-type *C. ochracea* ATCC 27872; Δ*sprT*, *sprT* ortholog-deficient *C. ochracea* mutant; Δ*sprB*, *sprB* ortholog-deficient *C. ochracea* mutant.

Fig. 6. Effects of *sprT* or *sprB* ortholog deficiency on biofilm stability. *Capnocytophaga ochracea* biofilms were incubated at 37°C under anaerobic conditions for 48 h and then washed a predetermined number of times. Black bar, 0 washes; white bar, 1 wash; light-gray bar, 3 washes. Percentages indicate the amount of biomass remaining after each wash as calculated by using the following equation: (Remaining biomass after each wash/biomass without washing) × 100. Data are presented as means ± SD (n = 18). *P < 0.05, **P < 0.01, ***P < 0.001 WT, wild-type *C. ochracea* ATCC 27872; Δ*sprT*, *sprT* ortholog-deficient *C. ochracea* mutant; Δ*sprB*, *sprB* ortholog-deficient *C. ochracea* mutant.

Fig. 7. Effect of enzyme treatment on the biofilms produced by *Capnocytophaga ochracea*. (A) Biofilms grown at 37 °C under anaerobic conditions for 48 h were treated with 0.5 mg/mL of proteinase K, DNase I, or sodium metaperiodate ($NaIO_4$) and then incubated

overnight at 37°C. After washing, the biofilms were stained with 0.1% crystal violet. Data are presented as means ± SD (n = 9). *P < 0.05, **P < 0.01, ***P < 0.001 (B) Representative photographs of the results of the crystal violet staining after enzymatic treatment of *C. ochracea* biofilms. WT, wild-type *C. ochracea* ATCC 27872; Δ*sprT*, *sprT* ortholog-deficient *C. ochracea* mutant; Δ*sprB*, *sprB* ortholog-deficient *C. ochracea* mutant.

Fig. 8. Effects of *gldK*, *sprT*, or *sprB* ortholog deficiency on the attachment of *Capnocytophaga ochracea* to a glass surface.

Number of cells attached to the cover slip was counted. Data are presented as means ± SD (n = 15). ***P < 0.001 WT, wild-type *C. ochracea* ATCC 27872; Δ*gldK*, *gldK* ortholog-deficient *C. ochracea* mutant; Δ*sprT*, *sprT* ortholog-deficient *C. ochracea* mutant; Δ*sprB*, *sprB* ortholog-deficient *C. ochracea* mutant.

Fig. 9. Model of the involvement of *C. ochracea* GldK, SprT, and SprB in attachment, gliding, and biofilms.

SprB is translocated to the cell surface and supernatant via the T9SS. Subsequently, SprB attaches to and gliding on solid surfaces. See text for details.

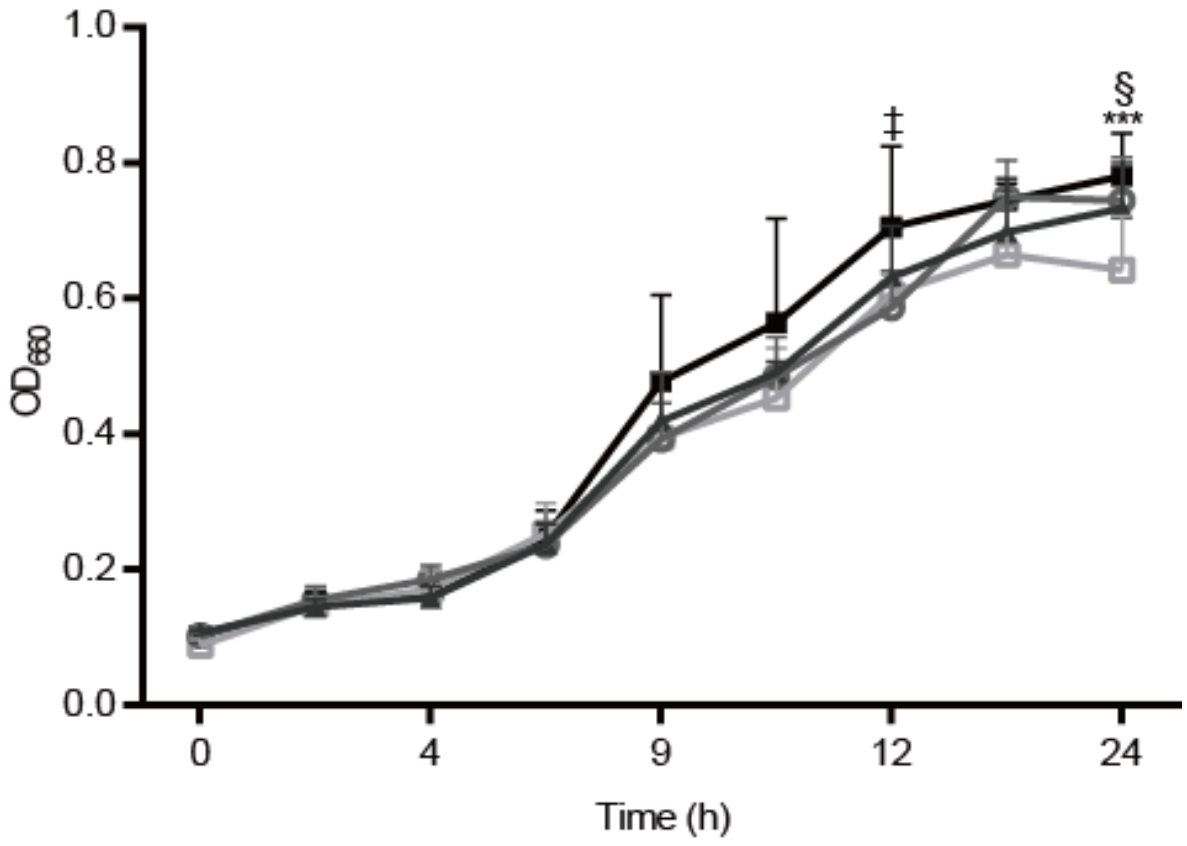

Fig. 1

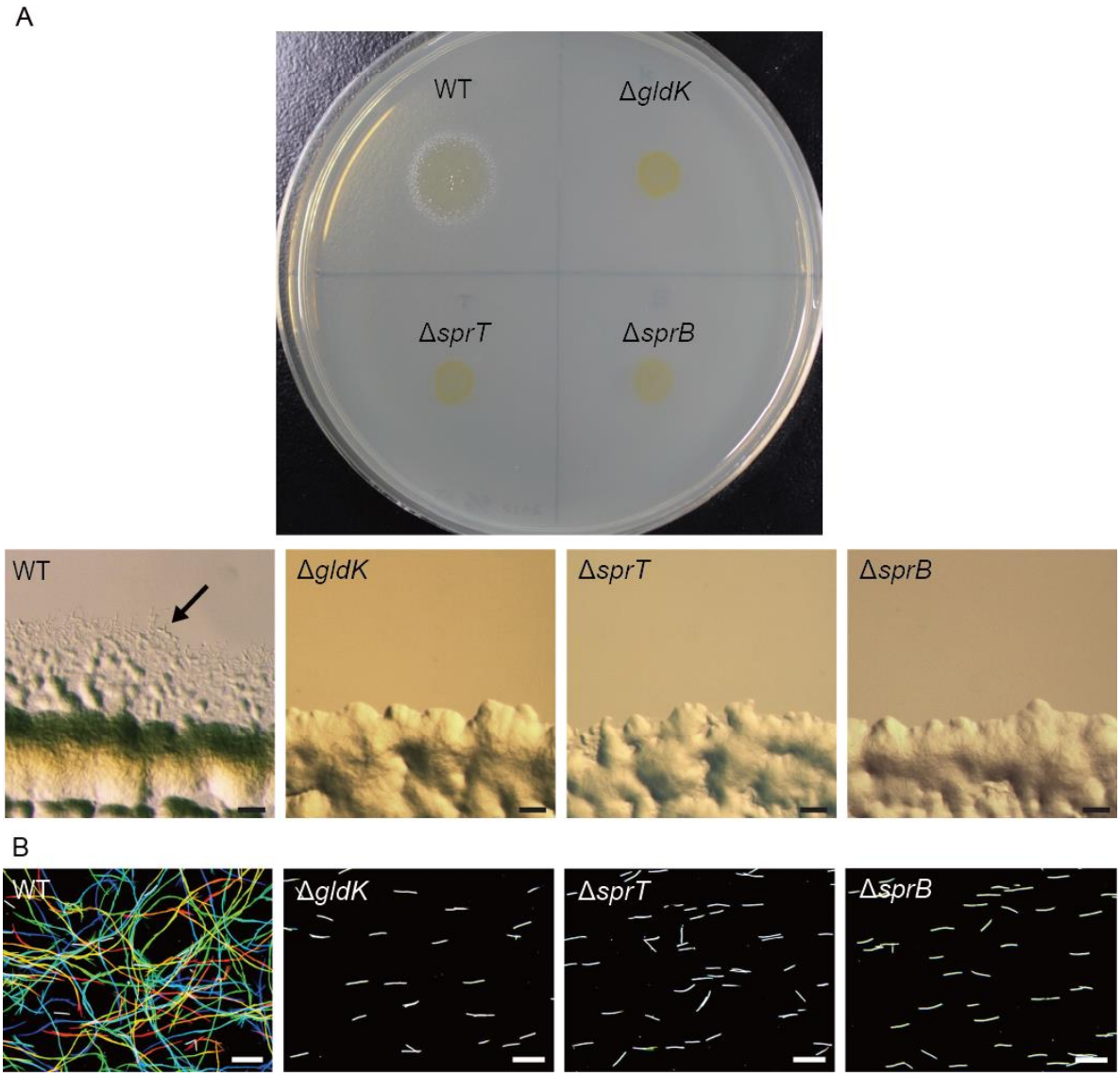
A
WT
ΔgldK
ΔsprT
ΔsprB
WT
ΔgldK
ΔsprT
ΔsprB
B
WT
ΔgldK
ΔsprT
ΔsprB

Fig. 2

Fig. 3

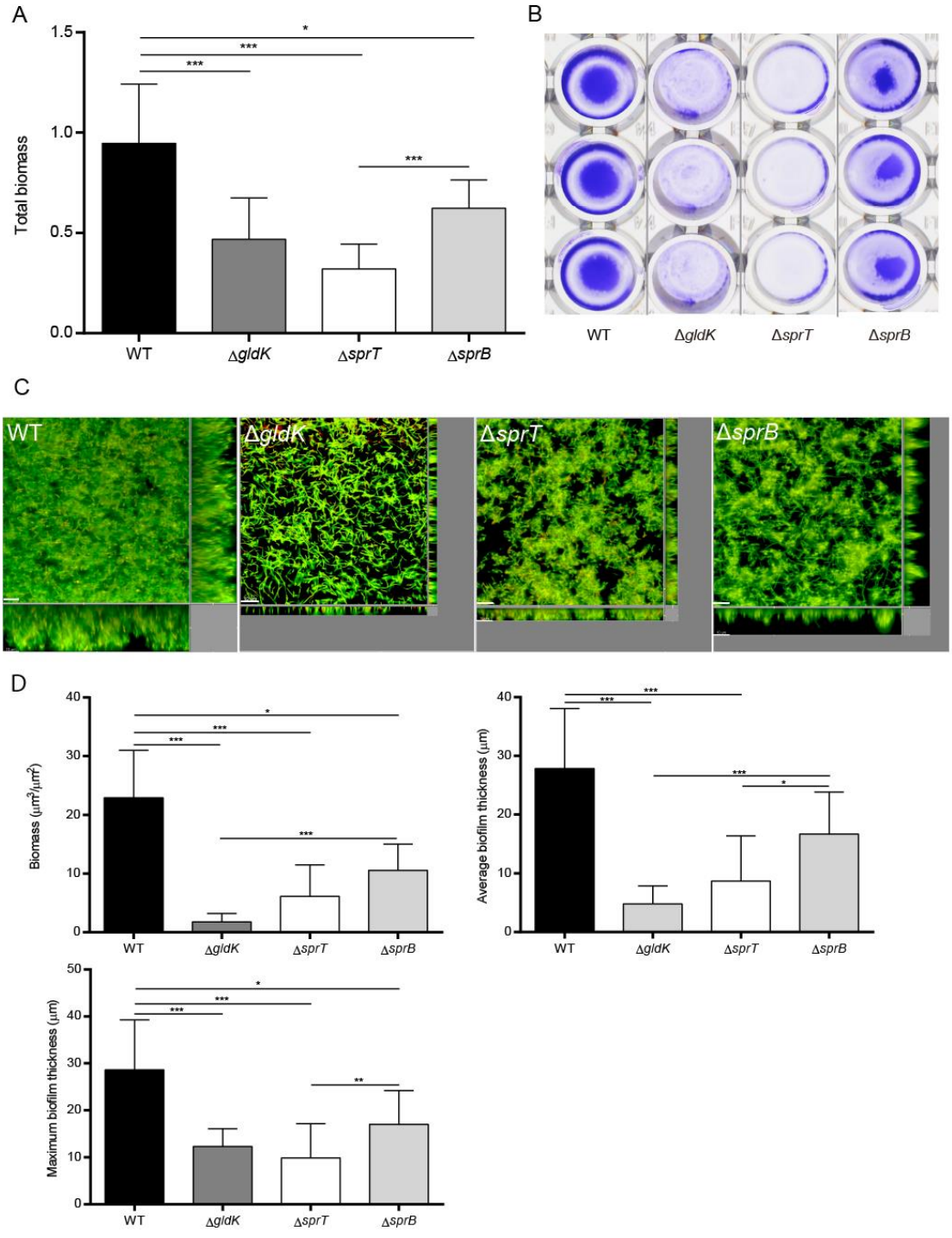
A
Total biomass
1.5
1.0
0.5
0.0
*
***
***
***
WT
ΔgldK
ΔsprT
ΔsprB
B
WT
ΔgldK
ΔsprT
ΔsprB
C
WT
ΔgldK
ΔsprT
ΔsprB
D
Biomass (μm³/μm²)
Average biofilm thickness (μm)
Maximum biofilm thickness (μm)
40
30
20
10
0
50
WT
ΔgldK
ΔsprT
ΔsprB

Fig. 4

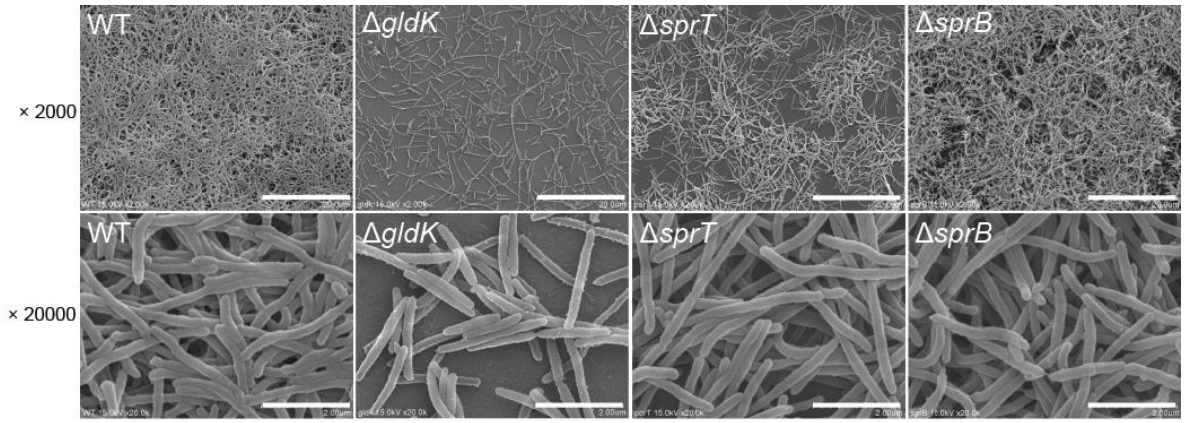

Fig. 5

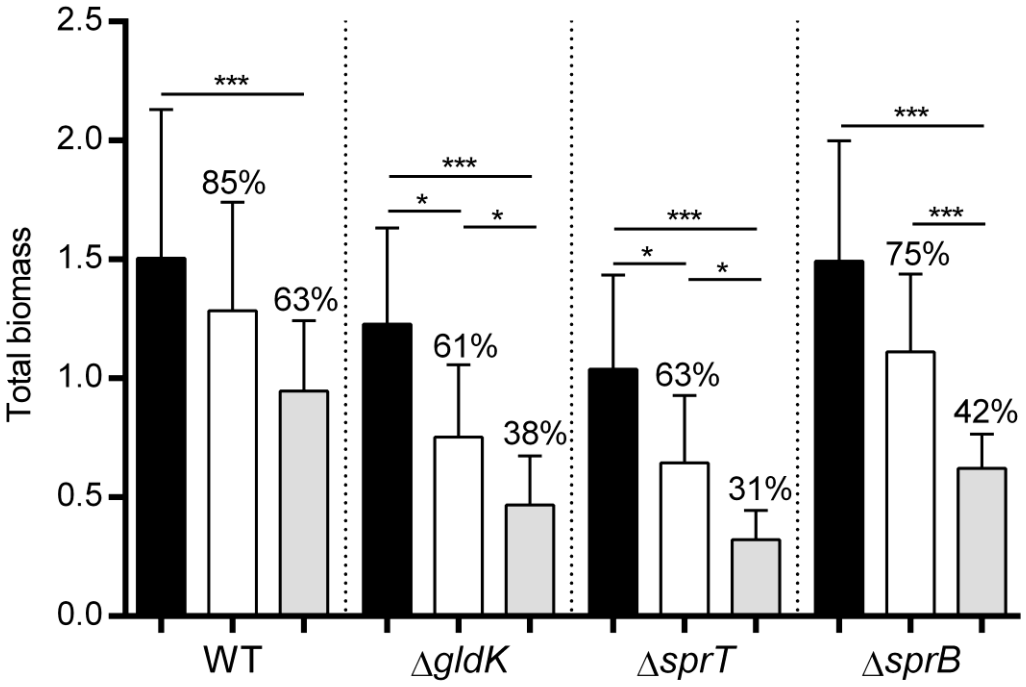
Total biomass
2.5
2.0
1.5
1.0
0.5
0.0
***
85%
63%
***
*
*
61%
38%
***
*
*
63%
31%
***
***
75%
42%
WT
ΔgldK
ΔsprT
ΔsprB

Fig. 6

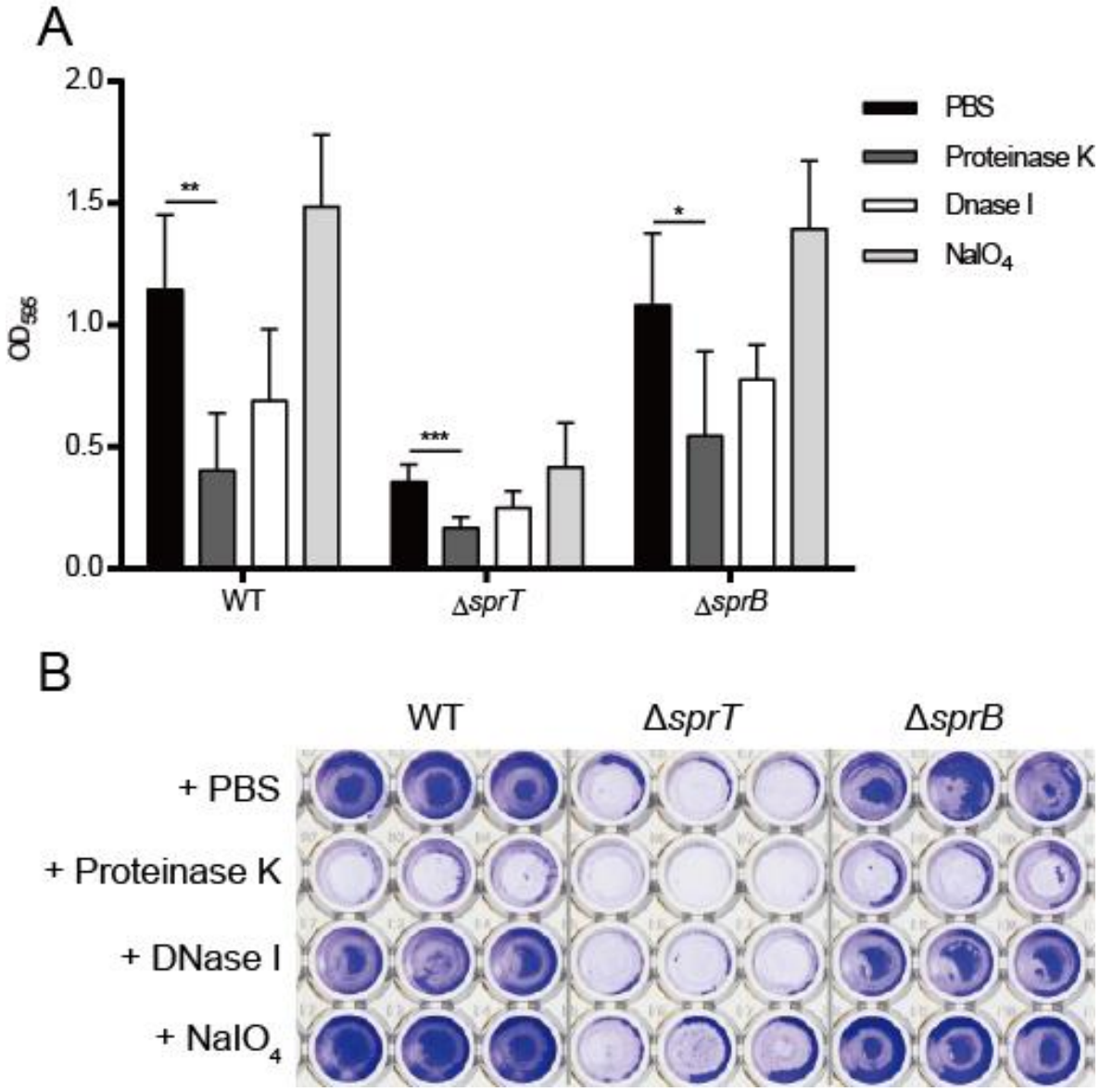
A
2.0
1.5
1.0
0.5
0.0
OD595
**
***
*
PBS
Proteinase K
Dnase I
NaIO4
WT
ΔsprT
ΔsprB
B
WT
ΔsprT
ΔsprB
+ PBS
+ Proteinase K
+ DNase I
+ NaIO4

Fig. 7

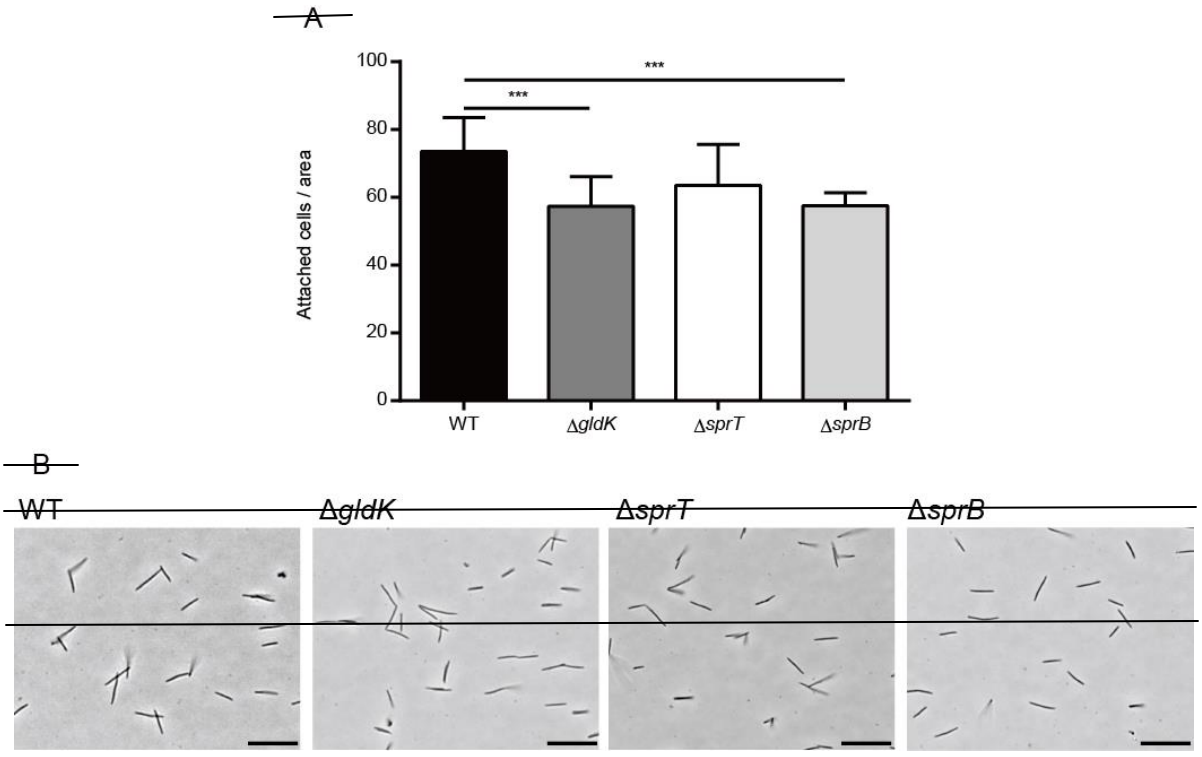
A
100
80
60
40
20
0
Attached cells / area
***
***
WT
ΔgldK
ΔsprT
ΔsprB
B
WT
ΔgldK
ΔsprT
ΔsprB

Fig. 8

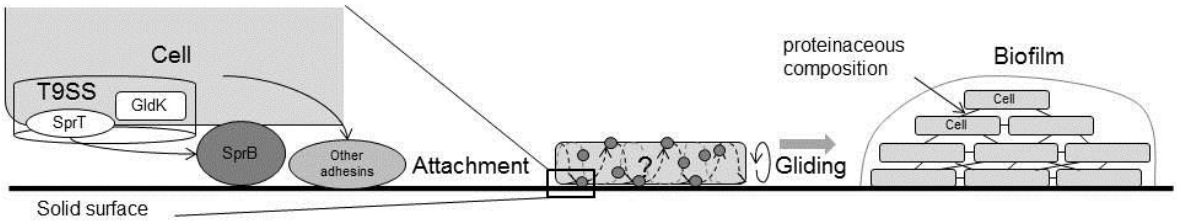
Cell
T9SS
GldK
SprT
SprB
Other adhesins
Attachment
?
Gliding
proteinaceous composition
Biofilm
Cell
Cell
Solid surface

Fig. 9

Table 1. Bacterial strains and plasmids used in the present study.

Strain or plasmid	Description[a]	Reference
Bacterial strains		
Escherichia coli DH5α	Strain used for gene cloning	TaKaRa Bio Inc.
Capnocytophaga ochracea strains		
ATCC 27872	Wild-type	ATCC
Δ*gldK* mutant	*ermF-ermAM* insertion mutation in Coch_0809 of ATCC 27872; Em^r	This study
Δ*sprT* mutant	*ermF-ermAM* insertion mutation in Coch_1748 of ATCC 27872; Em^r	This study
Δ*sprB* mutant	*ermF-ermAM* insertion mutation in Coch_0203 of ATCC 27872; Em^r	This study
Plasmids		
pVA2198	*ermF-ermAM*	27
pCR2.1-TOPO	3.9-kb vector for cloning PCR products; Km^r	Invitrogen

[a] Antibiotic resistance phenotypes: Km^r, kanamycin resistant; Em^r, erythromycin resistant.

Table 2. Primers used in the present study.

Primer	Sequence	Reference
SprT-F1	5' ACAGGATTAGATATCTCAGAAGGAA 3'	This study
SprT-R1	5' TGTTGCAAATACCGATGAGCTGCCCATACAAATTCAATGCTCCT 3'	This study
SprT-F2	5' CGTTACTAAAGGGAATGTAGCCCAATAGCCCTTGGACAAGTAACCTT 3'	This study
SprT-R2	5' CATTAGAAATGTTCTCGAATGAGAACTC 3'	This study
EMD2	5' GCTCATCGGTATTTGCAACATCATAG 3'	This study
EMU2	5' CTACATTCCCTTTAGTAACGTGTAACTTTC 3'	This study
SprB-F1	5' TTATAACGTAACGACTGACCCATTT 3'	This study
SprB-R1	5' AAGGGAATGTAGAATTATAGAGCTCAACGTGCCTATG 3'	This study
SprB-F2	5' ATACCGATGAGCAAAAGGAATATAATTCTGCCCAAAG 3'	This study
SprB-R2	5' ATCTACCACGAACAAGCGTATAGAG 3'	This study
EMSprB-F	5' AGCTCTATAATTCTACATTCCCTTTAGTAACGTGTAACTTTC 3'	This study
EMSprB-R	5' TATATTCCTTTTGCTCATCGGTATTTGCAACATCATAG 3'	This study
GldK-F1	5' GATGCCTACATTCAGTGTTGCCAAT 3'	This study
GldK-R1	5' TGTTGCAAATACCGATGAGCAGCTAGTACTAATAGTACAAGTAGCATTAC 3'	This study
GldK-F2	5' CGTTACTAAAGGGAATGTAGGCTCCTTACGGTATGACGCTTATTCCGAG 3'	This study
GldK-R2	5' TCATAGTAGACATATATTCATATGAATTCG 3'	This study

Underlined letters indicate overlap region.